Cosmological constraints without fingers of God

Mikhail M. Ivanov [1] [*] [a] **Oliver H. E. Philcox** [a,b,c] **Marko Simonović** [d] **Matias Zaldarriaga** [a] **Takahiro Nishimichi** [e,f] **Masahiro Takada** [f]

[a] *School of Natural Sciences, Institute for Advanced Study,*
1 Einstein Drive, Princeton, NJ 08540, USA

[b] *Department of Astrophysical Sciences, Princeton University,*
Princeton, NJ 08540, USA

[c] *Department of Applied Mathematics and Theoretical Physics, University of Cambridge,*
Cambridge CB3 0WA, UK

[d] *Theoretical Physics Department, CERN,*
1 Esplanade des Particules, Geneva 23, CH-1211, Switzerland

[e] *Center for Gravitational Physics,*
Yukawa Institute for Theoretical Physics, Kyoto University, Kyoto 606-8502, Japan

[f] *Kavli Institute for the Physics and Mathematics of the Universe (WPI), UTIAS*
The University of Tokyo, Kashiwa, Chiba 277-8583, Japan

ABSTRACT: Non-linear redshift-space distortions ("fingers of God") are challenging to model analytically, a fact that limits the applicability of perturbation theory in redshift space as compared to real space. We show how this problem can be mitigated using a new observable, Q_0, which can be easily estimated from the redshift space clustering data and is approximately equal to the real space power spectrum. The new statistic does not suffer from fingers of God and can be accurately described with perturbation theory down to $k_{\max} \simeq 0.4 \ h \ \mathrm{Mpc}^{-1}$. It can be straightforwardly included in the likelihood at negligible additional computational cost, and yields noticeable improvements on cosmological parameters compared to standard power spectrum multipole analyses. Using both simulations and observational data from the Baryon Oscillation Spectroscopic Survey, we show that improvements vary from 10% to 100% depending on the cosmological parameter considered, the galaxy sample and the survey volume.

---

[1] ivanov@ias.edu

[*] Einstein Fellow

Contents

1 Introduction

Reliable theoretical models for the intermediate- and short-scale galaxy power spectrum provide the key to obtaining tight constraints on cosmological parameters from current and future spectroscopic galaxy surveys [1–8]. In the analysis of the most recent Baryon Oscillation Spectroscopic Survey (BOSS) based on the Luminous Red Galaxy (LRG) sample [9], the main limiting factor in pushing to small scales are the non-linear redshift-space distortions, also known as the "fingers of God" (FoG) [10]. These non-linear effects contaminate the observed galaxy distribution along the line of sight $\hat{\mathbf{z}}$, even on relatively large scales. Further complications come from using the usual multipole expansion of the anisotropic redshift-space power spectrum, since it mixes modes that are parallel and perpendicular to $\hat{\mathbf{z}}$. As a result, FoGs, which affect only the modes along the line of sight, leaks into all power spectrum multipoles, significantly limiting the range of scales over which accurate modeling is possible.

In order to estimate the impact of FoGs, it is instructive to compare the range of validity of a given power spectrum model in real and redshift space. Recent analyses of the realistic mock catalogs simulating the BOSS galaxy sample show that the one-loop redshift space perturbation theory model breaks down at $k_{max} \simeq 0.25 \ h\mathrm{Mpc}^{-1}$ [3, 11, 12]. On the other hand, the real space data for the same volume can be well described by the one-loop model up to significantly smaller scales, $k_{max} \simeq 0.4 \ h\mathrm{Mpc}^{-1}$ [13, 14]. While these results depend on the survey volume, the effective redshift, and the type of tracers observed, they suggests that there is a potential to improve measurements of cosmological parameters by isolating FoG and extracting the information from the transverse Fourier modes (perpendicular to $\hat{\mathbf{z}}$) that are not affected by the non-linear redshift-space distortions.

Throughout the years, many methods had been proposed in order to achieve this goal. The most intuitive approach is to use the redshift-space power spectrum wedges [15, 16]. In Fourier space, such techniques effectively operate at the level of the anisotropic power spectrum $P(k, \mu)$, where $\mu \equiv \hat{\mathbf{k}} \cdot \hat{\mathbf{z}}$, and allow one to use a $\mu-$dependent k_{max} in the analysis [16]. While conceptually simple, the main shortcoming of wedges is that they cannot be efficiently estimated using FFT techniques, and in practice one has to estimate "pseudo wedges", obtained from the standard power spectrum multipoles [16]. Alternatively, several prescriptions have been used to "remove" FoGs directly at the map level [17–19], but it remains unclear if the additional systematic errors produced by such methods produce are too large for current and upcoming spectroscopic surveys [19].

In this paper, we build upon ideas from older works [17, 18, 20] and use a simple alternative statistic, dubbed Q_0. This is closely related to the real space power spectrum, and achieves the goal of isolating the FoG. In essence, this is obtained by measuring a particular linear combination of the first few power spectrum multipoles. The main advantages of Q_0 are the following: (a) It can be easily measured using conventional power spectrum multipole estimators; (b) Modulo small effects induced by the broadening of the BAO peak that affect only the BAO wiggles, Q_0 is equal to the real space power spectrum, and can be modeled to higher k_{max}; and (c) Its covariance matrix can be straightforwardly computed either analytically or from mock catalogs. Q_0 can thus be easily included in the galaxy power spectrum likelihood at negligible extra cost, opening up the possibility to partially include additional small-scale information and improve cosmological constraints compared to conventional power spectrum multipole analyses.

Before we dive into the details, it is worth pointing out the main difference in our approach compared to all previous work, which is related to reliably estimating the covariance for Q_0. The problem arises from the fact that the non-linear clustering generates all possible multipoles, whose covariance rapidly increases with the multipole order, ℓ. Therefore, if one attempts to produce a better estimate of the real space power spectrum using information from higher and higher ℓ, the estimator

quickly becomes very noisy, and essentially contains no information. This is clearly a paradox. In this work, we show how to resolve this issue and estimate Q_0 in a systematic fashion, while keeping the covariance under control. Our method is based on the theoretical error covariance approach [21, 22]. The key idea is to impose natural priors on the smoothness of the higher order multipoles, which, as we will show, effectively suppresses their contribution to the covariance of Q_0, while still contributing to the statistic itself. This approach allows multipoles up to arbitrary $\ell_{\max}$ to be included in the analysis if needed, guaranteeing the optimal error bars on Q_0.

Our paper is organized as follows. We begin with a preliminary discussion in Sec. 2, showing how Q_0 can be built from the usual Legendre multipoles with $\ell_{\max} = 4$ and discuss its relation to the real space power spectrum. Our approach is generalized to the case of general $\ell_{\max}$ in Sec. 3. Validation on large-volume N-body simulation data is given in Section 4, and applications to the real BOSS data and the DESI-like mocks shown in Section 5. Finally, we draw conclusions in Section 6. Some additional material is presented in Appendix A.

Throughout most of this paper, we will use the PT challenge simulation data [11], comprising BOSS-like mock catalogs with cumulative volume $\sim 566~(\text{Gpc}/h)^3$. For our purposes, we use only a single redshift bin with $z = 0.61$. We will describe the data from the mocks using one-loop perturbation theory templates, as implemented in the `CLASS-PT` code [14]. The parameter constraints are obtained with the `Montepython` MCMC sampler [23, 24] and analyzed using the `getdist` package [25].

2 Preliminary analysis

It is instructive to begin with a simplified example whereupon $P(k, \mu)$ is fully characterized by its first four moments, just as in linear theory [26]. In this instance, there is a simple rotation-like transformation between the moments of μ and the Legendre multipoles P_ℓ,

$$P(k, \mu) = \sum_{\ell=0,2,4} P_\ell(k)\mathcal{L}_\ell(\mu) = \sum_{n=0,2,4} Q_n(k)\mu^n \,, \tag{2.1}$$

where $\mathcal{L}_\ell$ is the Legendre polynomial of order ℓ. The power spectrum perpendicular to the line-of-sight, i.e. at $\mu = 0$, is given by Q_0. By definition, this coincides with the real-space galaxy power spectrum, which can be well described by the one-loop PT model up to $k_{\max} \sim 0.4~h\text{Mpc}^{-1}$ [13]. In contrast, the one-loop PT model for Q_2 and Q_4 breaks down on larger scales, since these moments are dominated by FoGs [3, 11, 14]. FoGs are a strong UV-effect that lowers the cutoff of the redshift-space effective field theory [27–29]. Indeed, estimates from the BOSS LRG sample give a redshift-space cutoff [1],

$$k_{\text{NL,FoG}} \approx \sigma_v^{-1} \simeq 0.25~h\text{Mpc}^{-1} \quad , \tag{2.2}$$

where σ_v is the short-scale velocity dispersion. This can be contrasted with the the cutoff of the real space effective field theory $k_{\rm NL,rs}$ (see Refs. [22, 30, 31]), which [21] estimate to be

$$k_{\rm NL,rs} \simeq 0.5 \ h{\rm Mpc}^{-1} \,. \tag{2.3}$$

Our goal is to extract the information contained in Q_0 while marginalizing over Q_2 and Q_4. An important problem is that the quantities measured by standard FFT power spectrum estimators are the multipoles (see e.g. [32–34]) and not the moments of μ. The multipoles pick up contributions from all moments, including those affected by FoG, i.e.

$$P_0 = Q_0 + \frac{1}{3}Q_2 + \frac{1}{5}Q_4 \,, \qquad P_2 = \frac{2}{3}Q_2 + \frac{4}{7}Q_4 \,, \qquad P_4 = \frac{8}{35}Q_4 \,. \tag{2.4}$$

However, given these simple linear relations, one can easily construct an estimator for Q_0 from the multipole estimators. Indeed, a straightforward estimator for Q_0 is given by the usual Scoccimarro-Yamamoto formula [33],

$$
\begin{aligned}
\check{Q}_0(k_i) &= \check{P}_0 - \frac{1}{2}\check{P}_2 + \frac{3}{8}\check{P}_4 \\
&= \frac{1}{V}\int_{k_i} \frac{d^3k}{4\pi k_i^2 \Delta k}\delta_0\left((2\cdot 0 + 1)\delta_0 - \frac{(2\cdot 2 + 1)}{2}\delta_2 + \frac{3(2\cdot 4 + 1)}{8}\delta_4\right) \,,
\end{aligned}
\tag{2.5}
$$

where V is the survey volume, $\int_{k_i}$ is the integral over the momentum shell of width Δk which is centered at k_i. Moreover, we have assumed the flat-sky approximation and the Kaiser limit [26] for the local redshift-space overdensity δ_ℓ, weighted with the appropriate Legendre polynomials,

$$\delta_\ell(k,\mu) \equiv (b_1 + f\mu^2)\delta_{\rm lin}(k)\mathcal{L}_\ell(\mu) \,. \tag{2.6}$$

In practice, if the measurements of $P_{0,2,4}$ are available, Q_0 can be constructed from this datavector by a simple linear summation of these multipoles with appropriate coefficients. The covariance matrix for Q_0 can be obtained directly from the estimator (2.5),

$$
\begin{aligned}
&\langle \check{Q}_0(k_i)\check{Q}_0(k_j)\rangle - \langle \check{Q}_0(k_i)\rangle\langle \check{Q}_0(k_j)\rangle \\
&= \frac{(2\pi)^3\delta_{ij}}{V 4\pi k_i^2 \Delta k}\int_0^1 d\mu \, P(k_i)^2(b_1 + f\mu^2)^4\left(\mathcal{L}_0(\mu) - \frac{2\cdot 2 + 1}{2}\mathcal{L}_2(\mu) + \frac{3}{8}(2\cdot 4 + 1)\mathcal{L}_4(\mu)\right)^2 \\
&= \frac{(2\pi)^3\delta_{ij}}{V 4\pi k_i^2 \Delta k}\left(\frac{225\check{P}_0^2}{64} - \frac{225\check{P}_0\check{P}_2}{88} + \frac{3775\check{P}_0\check{P}_4}{2288} + \frac{6975\check{P}_2^2}{9152} - \frac{775\check{P}_2\check{P}_4}{1144} + \frac{54975\check{P}_4^2}{155584}\right) \,.
\end{aligned}
\tag{2.7}
$$

Note that P_0 in the above formula contains the stochastic shot-noise term, equal to the inverse number density $\bar{n}^{-1}$ in the Poisson limit. The leading contribution to the covariance is given by the monopole moment (including the shot-noise),

$$\frac{2}{N_k}\frac{225P_0^2}{64} \simeq \frac{2}{N_k}3.5P_0^2 \,, \tag{2.8}$$

which is 3.5 times larger than the (auto-)covariance on the monopole, and ~ 4 times larger than the real space covariance (the additional increase is due to the Kaiser effect [26]). This apparent inflation of the error bars is driven by higher order multipoles P_2 and P_4, which are characterized by a large covariance. Thus, the large error on the reconstructed transverse moment Q_0 is the inevitable price of using the noisy Legendre multipoles in the estimator.

Alternatively, one can obtain the covariance matrix for Q_0 directly from the covariance matrix of the multipoles by an orthogonal transformation dictated by Eq. (2.4). Denoting this transformation as $P_\ell = M_{\ell n} Q_n$ (assuming Einstein summation conventions), we obtain

$$\hat{C}_{00}^{(Q)} = [(\hat{M}^T)_{0\ell} * \hat{C}_{\ell\ell'}^{-1} * \hat{M}_{\ell'0}]^{-1} = \hat{C}_{00} - \hat{C}_{02} + \frac{3\hat{C}_{04}}{4} + \frac{\hat{C}_{22}}{4} - \frac{3\hat{C}_{24}}{8} + \frac{9\hat{C}_{44}}{64}, \quad (2.9)$$

which reduces to Eq. (2.7) in the Gaussian approximation. For a realistic survey, the covariance of Q_0 can also be estimated from mock catalogs with the usual empirical estimator.
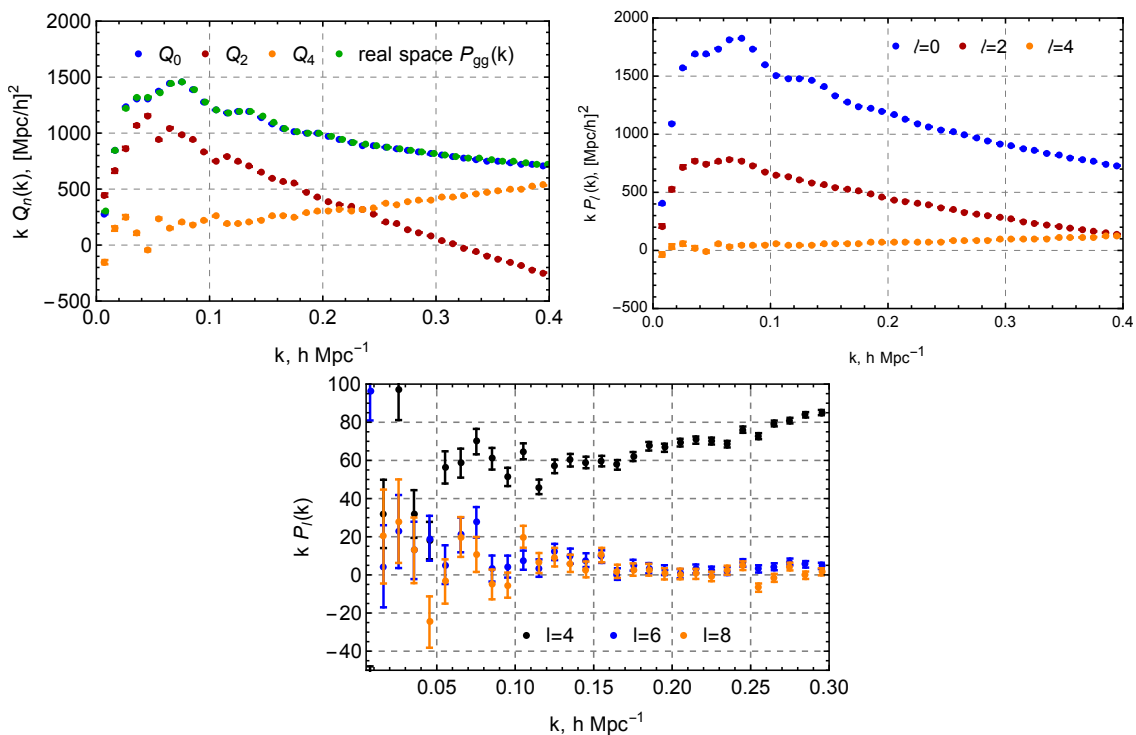

Figure 1. **Upper panel**: Comparison of moments, Q_n, and multipoles, P_ℓ, for the redshift-space power spectrum of PT challenge galaxies. The real space power spectrum P_{gg} (rescaled to match the AP effect present in Q_0) in the left plot is slightly shifted horizontally for clarity, as the datapoints overlap with those of Q_0. **Lower panel**: Higher-order Legendre multipoles with $\ell = 4, 6, 8$.

Let us consider the Q_n moments extracted from the PT challenge data, as shown in Fig. 1. Note that the PT challenge redshift space power spectrum moments P_ℓ are modulated by the Alcock-Paczynski (AP) effect [35], which is absent in the actual real space power spectrum P_{gg}, for which the comoving distances are computed using the true cosmology. In order to account for the difference between Q_0 and P_{gg}, we rescale the latter by the isotropic AP factor. As expected, we see that Q_0 is almost identical to the real space power spectrum, once the AP effect is taken into account. However, the higher moments Q_n vary quite significantly on mildly non-linear scales. In particular, Q_2 crosses zero at $k \simeq 0.3 \ h\mathrm{Mpc}^{-1}$, which may be interpreted as the PT breakdown for these moments: the zero-crossing means that the non-linear correction is comparable to the linear one. Moreover, non-linearities in the velocity field generate higher-order multipoles with $\ell > 4$. We show these multipoles (up to $\ell = 8$) estimated from the PT challenge data in the bottom panel of Fig. 1. In the presence of higher-order power spectrum multipoles, the estimator for Q_0 is given by (see Appendix A for a derivation):

$$\check{Q}_0 = \check{P}_0 - \frac{1}{2}\check{P}_2 + \frac{3}{8}\check{P}_4 - \frac{5}{16}\check{P}_6 + \frac{35}{128}\check{P}_8 + ... \tag{2.10}$$

In the next section we introduce a general formalism that allows one to take higher order multipoles into account consistently.

3 Formal derivation

In this Section, we will present a general formalism that allows one to reconstruct Q_0 from any survey for arbitrary $\ell_{\max}$. We saw in the previous section that using large $\ell_{\max}$ in the estimator of Q_0 leads to the inflation of the statistical errors since higher order Legendre multipoles have larger variances. However, one can imagine a situation in which the survey volume is such that these moments can become important, and their exclusion can lead to noticeable systematic errors. To include Q_0 for an arbitrary $\ell_{\max}$, it is more convenient to re-derive the previous results using a different approach, which we present here.

3.1 The case of $\ell_{\max} = 4$

Let us start again with the familiar case $\ell_{\max} = 4$ and consider the likelihood for power spectrum multipoles in the Gaussian diagonal approximation,

$$-2\ln L(Q_0, Q_2, Q_4) = \Delta\vec{P}_\ell \cdot \hat{C}_{\ell\ell'}^{-1} \cdot \Delta\vec{P}_{\ell'}, \quad \text{where}$$
$$\Delta\vec{P}_0 = \left(Q_0(k_i) + \frac{1}{3}Q_2(k_i) + \frac{1}{5}Q_4(k_i) - P_0^{\mathrm{data}}(k_i)\right),$$
$$\Delta\vec{P}_2 = \left(\frac{2}{3}Q_2(k_i) + \frac{4}{7}Q_4(k_i) - P_2^{\mathrm{data}}(k_i)\right), \tag{3.1}$$
$$\Delta\vec{P}_4 = \left(\frac{8}{35}Q_4(k_i) - P_4^{\mathrm{data}}(k_i)\right),$$

where we have suppressed the explicit summation over multipoles and and wavenumber indices.

In the Gaussian approximation all k-bins are independent. Thus, we can consider the likelihood for each bin separately. Marginalizing the likelihood (3.1) for the i-th bin over Q_2 and Q_4 we obtain we following reduced likelihood:[1]

$$- 2 \ln L_{\text{marg.}}(Q_0) = \sum_{i=1}^{N_{\text{bins}}} \frac{(P_0^{\text{data}}(k_i) - \frac{1}{2}P_2^{\text{data}}(k_i) + \frac{3}{8}P_4^{\text{data}}(k_i) - Q_0(k_i))^2}{C_{00} - C_{02} + \frac{3C_{04}}{4} + \frac{C_{22}}{4} - \frac{3C_{24}}{8} + \frac{9C_{44}}{64}}, \quad (3.2)$$

which exactly coincides with the likelihood for Q_0 from the previous section. Clearly, this derivation has allowed too much freedom: we have marginalized over Q_2 and Q_4 allowing independent and arbitrarily large fluctuations in every k-bin. However, we expect that the scale-dependent FoG contributions are smooth finite functions. This condition can be implemented by means of the prior on the (unknown) full theoretical model, along the lines of Ref. [21].

3.2 Warmup: theoretical prior on the quadrupole

Next, let us discuss how the likelihood for Q_0 changes if we include some prior information on the power spectrum multipoles. Our derivation will closely follow the derivation of the covariance matrix in the theoretical error formalism [21]. For simplicity, let us consider a situation in which the redshift-space power spectrum depends only on the two moments, Q_0 and Q_2. We need to marginalize this likelihood over Q_2. Repeating the derivation above, we find following likelihood for Q_0 alone:

$$- 2 \ln L(Q_0) = \sum_{i=1}^{N_{\text{bins}}} \frac{(P_0^{\text{data}}(k_i) - P_2^{\text{data}}(k_i)/2 - Q_0(k_i))^2}{C_{00}(k_i) - C_{02}(k_i) + C_{22}(k_i)/4}. \quad (3.3)$$

We now assume that there is some prior knowledge of the expectation value $\bar{P}_2$ with some error E_i. In other words, there is a likelihood for the theoretical prediction of $\bar{P}_2$,

$$- 2 \ln L_{\text{E}} = (P_2[Q_2] - \bar{P}_2) \cdot \hat{C}_{(P_2)}^{-1} \cdot (P_2[Q_2] - \bar{P}_2) = (\Delta\vec{Q}_2 - \Delta\vec{Q}_2') \cdot \hat{\Psi}^{(E)} \cdot (\Delta\vec{Q}_2 - \Delta\vec{Q}_2'),$$
$$\Delta\vec{Q}_2 = \vec{Q}_2 - \vec{Q}_2^{\text{data}}, \quad \Delta\vec{Q}_2' = \bar{\vec{Q}}_2 - \vec{Q}_2^{\text{data}},$$
$$(3.4)$$

where the second equality has rewritten the likelihood for P_2 in terms of the likelihood for Q_2, using $\bar{Q}_2 \equiv 3\bar{P}_2/2$ and defining some precision matrix $\hat{\Psi}^{(E)}$. The split into

---

[1]For simplicity, we will ignore the logarithmic corrections to the marginalization result in what follows. The leading effect of these corrections is to change the likelihood normalization, which can be neglected in MCMC analysis.

$\Delta \vec{Q}_2$ and $\Delta \vec{Q}'_2$ will be clear shortly. Note that, in principle, the covariance $C_{(P_2)}^{-1}$ is fully correlated. The total likelihood takes the following form,

$$
\begin{aligned}
-2\ln L(Q_0, Q_2) &= \sum_{i=1}^{N_{\rm bins}} \Delta \vec{P}_\ell C_{\ell\ell'}^{-1} \Delta \vec{P}_{\ell'} + \sum_{i,j}^{N_{\rm bins}} C_E^{-1}(P_2[Q_2](k_i) - \bar{P}_2(k_i))(P_2[Q_2](k_j) - \bar{P}_2(k_j)), \\
&= \Delta \vec{Q}_m \cdot \hat{\Psi}_{mn} \cdot \Delta \vec{Q}_n + \Delta \vec{Q}_2 \cdot \hat{\Psi}^{(E)} \cdot \Delta \vec{Q}_2.
\end{aligned}
\tag{3.5}
$$

The likelihood marginalized over Q_2 can be easily obtained,

$$
\begin{aligned}
&-2\ln L(Q_0) = \\
&(\Delta \vec{Q}_0 + \{\hat{\Psi}_{00} - \hat{\Psi}_{02}(\hat{\Psi}_{22} + \hat{\Psi}^{(E)})^{-1}\hat{\Psi}_{02}\}^{-1}(\hat{\Psi}_{02}(\hat{\Psi}_{22} + \hat{\Psi}^{(E)})^{-1}\hat{\Psi}^{(E)} \cdot \Delta \vec{Q}'_2)) \\
&\times \left(\hat{\Psi}_{00} - \hat{\Psi}_{02}(\hat{\Psi}_{22} + \hat{\Psi}^{(E)})^{-1}\hat{\Psi}_{02}\right) \\
&\times (\Delta \vec{Q}_0 + \{\hat{\Psi}_{00} - \hat{\Psi}_{02}(\hat{\Psi}_{22} + \hat{\Psi}^{(E)})^{-1}\hat{\Psi}_{02}\}^{-1}(\hat{\Psi}_{02}(\hat{\Psi}_{22} + \hat{\Psi}^{(E)})^{-1}\hat{\Psi}^{(E)} \cdot \Delta \vec{Q}'_2)).
\end{aligned}
\tag{3.6}
$$

To obtain some insight into the structure of this likelihood, we use several approximations. First, let us neglect the cross-covariance C_{02} between the multipoles; this is reasonable since the normalized correlation coefficient is typically small, $r_{02} = C_{02}/(C_{00}^{1/2} C_{22}^{1/2}) \sim 0.1 \ll 1$ for the PT Challenge mocks. Note that the prediction matrix is not diagonal, i.e. $\hat{\Psi}_{02}$ is still non-trivial in this approximation, with

$$
\hat{\Psi}_{02} = \hat{C}_{00}^{-1}/3.
\tag{3.7}
$$

As a second approximation, we consider the asymptotic regime $C_E/C \to \infty$. This corresponds to very poor prior knowledge about $\bar{P}_2$. In this limit, the terms with the theoretical error drop out and, to leading order in $\mathcal{O}((C_E/C)^{-1})$, we obtain

$$
\begin{aligned}
&-2\ln L(Q_0) = \\
&= (P_0^{\rm data} - P_2^{\rm data}/2 - Q_0) \cdot \left(\hat{\Psi}_{00} - \hat{\Psi}_{02}\hat{\Psi}_{22}^{-1}\hat{\Psi}_{02}\right) \cdot (P_0^{\rm data} - P_2^{\rm data}/2 - Q_0) \\
&= \sum_{i=1}^{N_{\rm bins}} \frac{(P_0^{\rm data} - P_2^{\rm data}/2 - Q_0)^2}{C_{00} + C_{22}/4}\bigg|_{k_i},
\end{aligned}
\tag{3.8}
$$

where in the last line we have implemented the Gaussian approximation. Eq. (3.8) gives a usual likelihood with the variance on the estimator $\hat{Q}_0 = P_0 - P_2/2$ reconstructed from the monopole and the quadrupole. In the opposite limit $C_E/C \to 0$, where the theoretical prior is infinitely precise, we have

$$
-2\ln L(Q_0) = \sum_{i=1}^{N_{\rm bins}} \frac{(Q_0 - P_0^{\rm data} + \bar{P}_2/2)^2}{C_{00}} + \mathcal{O}(C_E).
\tag{3.9}
$$

As expected, at leading order in $C^{(E)}$ adding the prior knowledge on P_2 is analogous to fitting the Q_0 moment constructed with the prior prediction $\bar{P}_2$, i.e.

$$\hat{Q}_0 = P_0 - \frac{1}{2}\bar{P}_2 \,. \tag{3.10}$$

Importantly, in this case one does not pay the price of including (noisy) P_2 in the estimator for $\hat{Q}_0$, i.e. the covariance is given only by the monopole contribution.

3.3 Generalization to higher order multipoles

Generalization is straightforward, and takes the form

$$
\begin{aligned}
- 2 \ln L(Q_0, ..., Q_{\ell_{\max}}) = &\sum_{i=1}^{N_{\mathrm{bins}}} \sum_{\ell, \ell' \le \ell_{\max}} C^{-1}_{\ell\ell' \,\mathrm{data}} \Delta P_\ell \Delta P_{\ell'} \\
&+ \sum_{\ell=0}^{\ell_{\max}} \sum_{i,j}^{N_{\mathrm{bins}}} (P_\ell[Q](k_i) - \bar{P}_\ell(k_i))(\hat{C}^{(\mathrm{E}),\,(\ell\ell')})^{-1}_{ij}(P_\ell[Q](k_j) - \bar{P}_\ell(k_j)) \,,
\end{aligned}
\tag{3.11}
$$

where $P_\ell[Q]$ denotes a general expression for the power spectrum multipole ℓ through moments of μ (see Appendix A). The prior $\bar{P}_\ell$ can be either a fit to the data with some smooth function, or taken from the perturbation theory prediction. For $\ell > 4$ either option gives an envelope very close to 0 on mildly non-linear scales. The final likelihood for Q_0 is obtained by marginalizing (3.11) over all Q_ℓ functions with $\ell \ge 2$, which can be performed analytically. In general, smoothness in μ and k implies that the prior covariance should be 100% correlated [14]:

$$C^{(\mathrm{E}),\,(\ell\ell')}_{ij} = E_\ell(k_i) E_{\ell'}(k_j) \,. \tag{3.12}$$

However, given that the true shape is not known, we impose a weaker condition on smoothness in μ and k-space. Namely, we will use [22]

$$C^{(\mathrm{E}),\,(\ell\ell')}_{ij} = E_\ell(k_i) E_{\ell'}(k_j) \exp\left(-\frac{(k_i - k_j)^2}{2\Delta k^2}\right) \exp\left(-\frac{(\ell - \ell')^2}{2\Delta\ell^2}\right) \,. \tag{3.13}$$

Conservatively, we can choose the theory prior to be 100% of the expected value, e.g.

$$E_\ell(k_i) = \bar{P}_\ell(k_i) \,. \tag{3.14}$$

The full likelihood (3.11) simplifies in the two extreme limits, $C_E \ll C_{\mathrm{data}}$ and $C_E \gg C_{\mathrm{data}}$. As we have seen in the previous section, in the first case one need simply replace the true datavector P_ℓ by $\bar{P}_\ell$ in the estimator of $\hat{Q}_0$. This does not require any change to the covariance, hence we do not pay the price of using the noisy P_ℓ in our Q_0 estimator. In the second case we must use the P_ℓ from the data when constructing $\hat{Q}_0$ and include the noise of this multipole in our covariance. For all practical purposes it is sufficient to work within these two limits. To estimate the

transition between the two regimes, we may compare the effective χ^2 contribution coming from the data and the prior on P_ℓ:

$$\chi^2_{\text{data}} = (\vec{P}_\ell - \bar{\vec{P}}_\ell) \cdot \hat{C}^{-1}_{\ell\ell} \cdot (\vec{P}_\ell - \bar{\vec{P}}_\ell)$$
$$\chi^2_{\text{prior}} = (\vec{P}_\ell - \bar{\vec{P}}_\ell) \cdot (\hat{C}^{(E)}_{(\ell\ell')})^{-1} \cdot (\vec{P}_\ell - \bar{\vec{P}}_\ell)$$

(3.15)

This suggests the following algorithm to deal with multipoles $\ell \geq 4$:

1. Select some $\ell_{\text{max}} \geq 4$ and estimate all mutipoles with $\ell \leq \ell_{\text{max}}$. Fit these multipoles with some smooth curves $\bar{P}_\ell$.

2. For each $4 \leq \ell \leq \ell_{\text{max}}$ compute the ratio $\chi^2_{\text{data}}/\chi^2_{\text{prior}}$. If $\chi^2_{\text{data}}/\chi^2_{\text{prior}} > 1$, P_ℓ should be included in the Q_0 estimator along with its effect on the covariance. In the opposite regime, $\check{Q}_0$ and its covariance should be estimated using only the lower multipoles. For all higher multipoles, add the contribution from the relevant multipole moment ℓ as a smooth prior $\bar{P}_\ell$ to $\check{Q}_0$.

3.4 Modelling Q_0

Finally, let us discuss the theoretical model for Q_0. In linear theory, Q_0 would be the real space galaxy auto power spectrum P_{gg}. The situation becomes more complicated when IR resummation (i.e. the effects of long-wavelength displacements, which cannot be treated perturbatively) is taken into account. Indeed, the non-linear BAO damping factor is direction-dependent [36]. Assuming a wiggly-smooth decomposition of the linear power spectrum $P_{\text{lin}} = P_{\text{nw}} + P_{\text{w}}$ [37–40], at leading order we may write

$$P(k,\mu) = (b_1 + f\mu^2)^2 \left(P_{\text{nw}} + P_{\text{w}} e^{-\Sigma^2 k^2 (1+f\mu^2(2+f)) - \delta\Sigma^2 k^2 f^2 \mu^2 (\mu^2-1)} \right), \qquad (3.16)$$

where the BAO damping functions are given by

$$\Sigma^2 = \frac{1}{6\pi^2} \int_0^{k_S} dq\, P_{\text{nw}}(q)(1 - j_0(qr_{\text{BAO}}) + 2j_2(qr_{\text{BAO}})),$$
$$\delta\Sigma^2 = \frac{1}{2\pi^2} \int_0^{k_S} dq\, P_{\text{nw}}(q) j_2(qr_{\text{BAO}}),$$

(3.17)

for spherical Bessel functions $j_\ell(x)$, comoving BAO scale at the drag epoch r_{BAO}, and separation scale k_S. Since the damping factor is large, the exponential suppression cannot be Taylor-expanded. This means, that, in general, we need to use an infinite series in P_ℓ in our estimator of Q_0 in order to remove the direction-dependence of the BAO wiggles. However, as the shape of the BAO wiggles is known analytically to all orders in μ, we can just compute redshift-space multipoles, $\{P_\ell\}$, theoretically and then combine them into Q_0 just as for the data. This guarantees that the suppression

of the BAO wiggles in Q_0 is the same in the datavector and in the theory model. Thus, our theory model is

$$Q_0(k) = P_0(k) - \frac{1}{2}P_2(k) + \frac{3}{8}P_4(k) \,, \qquad (3.18)$$

where $P_{0,2,4}$ contain all necessary redshift-space counterterms. The priors on these counterterms can be extracted from fitting the full datavector $P_{0,2,4}$ at low k_{max}, where the perturbative modeling of FoGs is still accurate.
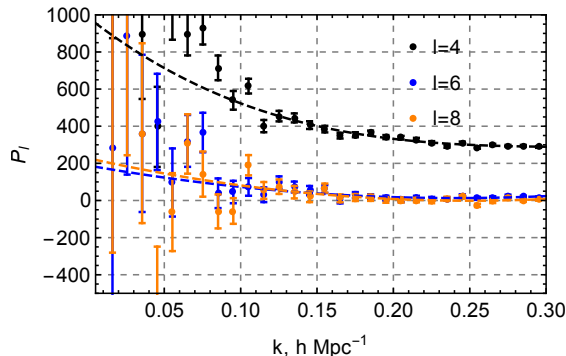
Figure 2. Higher order multipoles of the PT challenge data and their fits by quadratic polynomials.

4 Validation on PT challenge mocks

In this section we apply the formalism described above to the PT challenge data. We will use the Gaussian approximation for all sample covariance matrices, which has been shown to be very accurate for the purpose of parameter constraints [41].

4.1 Estimation of Q_0 from the data

As a first step, we obtain an estimate for $\bar{P}_\ell$ from the fits to the data, as in the left panel of Fig. 2. As a second step, we compute $\chi^2_{\text{data}}/\chi^2_{\text{prior}}$ assuming the following 100% prior on P_ℓ:

$$C_{ij}^{(\text{E})\ (\ell\ell')} = \bar{P}_\ell(k_i)\bar{P}_{\ell'}(k_j)\exp\left(-\frac{(k_i - k_j)^2}{2\Delta k^2}\right)\exp\left(-\frac{(\ell - \ell')^2}{2\Delta\ell^2}\right) \,, \qquad (4.1)$$

The coherence length Δk characterizes the amount of correlation across different k-bins, and ensures that the likelihood properties do not depend on the binning. Choosing a large Δk increases the significance of the theoretical prior by assuming an extra correlation between k bins. The coherence in ℓ space corresponds to a smoothness of the power spectrum as a function of μ. In practice, we choose $\Delta k = 0.001\ h/\text{Mpc}$ and assume also that the theoretical prior covariance matrix is diagonal

in the multipole space, i.e. $\Delta \ell = 0$. This choice corresponds to a very conservative situation where the prior on $\bar{P}_\ell$ is quite poor. Essentially, we do not require the 2D power spectrum prior $P(k, \mu)$ to be a smooth function in both k and μ. Even this very conservative situation will be sufficient for our purposes. With our choice of Δk and $\Delta \ell$, and using $k_{\max} = 0.3 \ h/\mathrm{Mpc}$, we find

$$\frac{\chi^2_{\mathrm{prior}}}{\chi^2_{\mathrm{data}}} = 0.9, \ 80, \ 75 \quad \text{for} \quad \ell = 4, \ 6, \ 8 \,. \tag{4.2}$$

One can also check that $\chi^2_{\mathrm{prior}}/\chi^2_{\mathrm{data}} \ll 1$ is always true for $\ell = 0, 2$. For a more aggressive choice of $\Delta k = 0.01 \ h\mathrm{Mpc}^{-1}$ we obtain the following numbers:

$$\frac{\chi^2_{\mathrm{prior}}}{\chi^2_{\mathrm{data}}} = 2, \ 232, \ 196 \quad \text{for} \quad \ell = 4, \ 6, \ 8 \,, \tag{4.3}$$

which do not change results qualitatively. These results suggests that our prior is marginally important for $\ell = 4$, and it is much more significant than the actual likelihood contribution for $\ell > 4$. If we include off-diagonal-in-ℓ matrix elements, which correspond to a prior on the smoothness of the power spectrum in μ, the significance of the priors will increase even further. In particular, for $\Delta \ell = 2$ we have:

$$\frac{\chi^2_{\mathrm{prior}}}{\chi^2_{\mathrm{data}}} = 3.3, \ 152 \quad \text{for} \quad \ell = 4, \ 6 \,. \tag{4.4}$$

On the one hand, the $\ell = 4$ prior never dominates over the data by more than a factor of few, regardless of the set-up. To be maximally conservative, we will always include the hexadecapole in our analysis and take into account its contribution into the covariance matrix. On the other hand, we see that the contribution of higher order multipoles ($\ell > 4$) is always dominated by priors. Thus, we conclude that even for the large-volume PT challenge mocks the higher-order multipole moments $\ell > 4$ can be ignored in the estimation of the covariance matrix for Q_0 in the mildly non-linear regime. However, we may want to include higher multipoles in the form of the mean prior to the theoretical model. To this end, we need to check if their inclusion is strictly needed to describe the data. To that end, we perform several MCMC analyses of the Q_0 likelihood from the PT challenge data for different choices of $\ell_{\max}$.

We fit the joint likelihood comprising the multipoles $P_{0,2,4}$ for $k_{\max} = 0.14 \ h\mathrm{Mpc}^{-1}$ and Q_0 in the range $0.14 \ h\mathrm{Mpc}^{-1} \leq k < 0.3 \ h\mathrm{Mpc}^{-1}$. Since the k-bins do not overlap between the two likelihoods do not overlap, they are uncorrelated in the Gaussian limit. We fit $P_{0,2,4}$ datavector with the one-loop effective field theory template of Refs. [3, 11, 14, 29]. Note that we include the next-to-leading order operator $\tilde{c} k^4 \mu^4 P_{\mathrm{lin}}(k)$ in our analysis to account for higher-order FoG effects. Additionally, we

use the full set of stochastic contributions from Refs. [29, 42],

$$P_{\text{stoch}}(k, \mu) = \left\{ a_0 \left(\frac{k}{k_{\text{NL}}} \right)^2 + a_2 \mu^2 \left(\frac{k}{k_{\text{NL}}} \right)^2 + P_{\text{shot}} \right\} \cdot \frac{1}{\bar{n}} \, [\text{Mpc}/h]^3 \,, \qquad (4.5)$$

where $\bar{n}$ is the inverse number density of tracers. Using the hexadecapole moment we are able to break the strong degeneracy between a_2 and $\tilde{c}$, which is present in the $P_{0,2}$ likelihood. As to Q_0, we use the model (3.18), which depends on the same nuisance parameters as our likelihood for the multipoles for $k_{\text{max}} = 0.14 \, h/\text{Mpc}$. We use the following parameter vector (see [14] for our notations):

$$\{\omega_m, h, A_s\} \times \{b_1, b_2, b_{\mathcal{G}_2}, b_{\Gamma_3}, c_0, c_2, c_4, \tilde{c}, a_0, a_2, P_{\text{shot}}\} \,. \qquad (4.6)$$

We fix n_s and Ω_b/Ω_m to the known fiducial values as in Ref. [11]. The following Gaussian priors on the nuisance parameters are assumed:

$$a_0 \sim \mathcal{N}(0, 1^2) \quad a_2 \sim \mathcal{N}(0, 1^2) \quad P_{\text{shot}} \sim \mathcal{N}(0, 0.3^2) \,, \quad b_{\Gamma_3} \sim \mathcal{N} \left(\frac{23}{42}(b_1 - 1), 1^2 \right) \,, \qquad (4.7)$$

using flat infinite priors on $b_1, b_2, c_0, c_2, c_4, \tilde{c}$ and $b_{\mathcal{G}_2}$. The mean value of b_{Γ_3} is taken from the prediction of the coevolution model [43, 44]. Since the Poissonian shot noise contribution was subtracted from the data, we assume that the mean residual contribution is zero, with variance corresponding to $\sim 30\%$ of $\bar{n}^{-1}$, consistent with the deviations due to the halo exclusions [13, 45] expected for the BOSS-like host halos.

Let us now study the convergence of our method with respect to the value of the maximal multipolar index. In particular, we consider $\ell_{\text{max}} = 4, 6, 8$. In all cases, the hexadecapole is fully included in the theory, data and the covariance, with $\ell = 6, 8$ included only via priors. The results of our analysis are shown in Fig. 3 and Table 1. Each parameter p (except b_2 and $b_{\mathcal{G}_2}$) is shown in the format $\Delta p/p \equiv p/p_{\text{true}} - 1$, where we use fiducial values for true cosmological parameters, and extract the true value of b_1 from the galaxy-matter cross spectrum [11]. For b_2 and $b_{\mathcal{G}_2}$ we use the format $\Delta p \equiv p - p_{\text{true}}$, where the true values of b_2 and $b_{\mathcal{G}_2}$ are measured from the combined power spectrum and bispectrum analysis [46]. For comparison, we show also the baseline results for the $P_{0,2}$ likelihood at $k_{\text{max}} = 0.14 \, h/\text{Mpc}$. On the one hand, we can see that Q_0 narrows the contours for the ω_m and H_0 by $\lesssim 20\%$. This improvement is expected since these parameters are measured from the shape of Q_0. In contrast, the amplitude parameters $A^{1/2}$ and σ_8 cannot be accurately measured from the real-space galaxy power spectrum alone because of the degeneracy with galaxy bias. This explains why the posteriors for these parameters do not appreciably shrink after the inclusion of Q_0. The priors on higher order multipoles in the estimator $\check{Q}_0$ have a negligible effect on the posterior distribution, which motivates us to use $\ell_{\text{max}} = 4$ as our baseline choice.
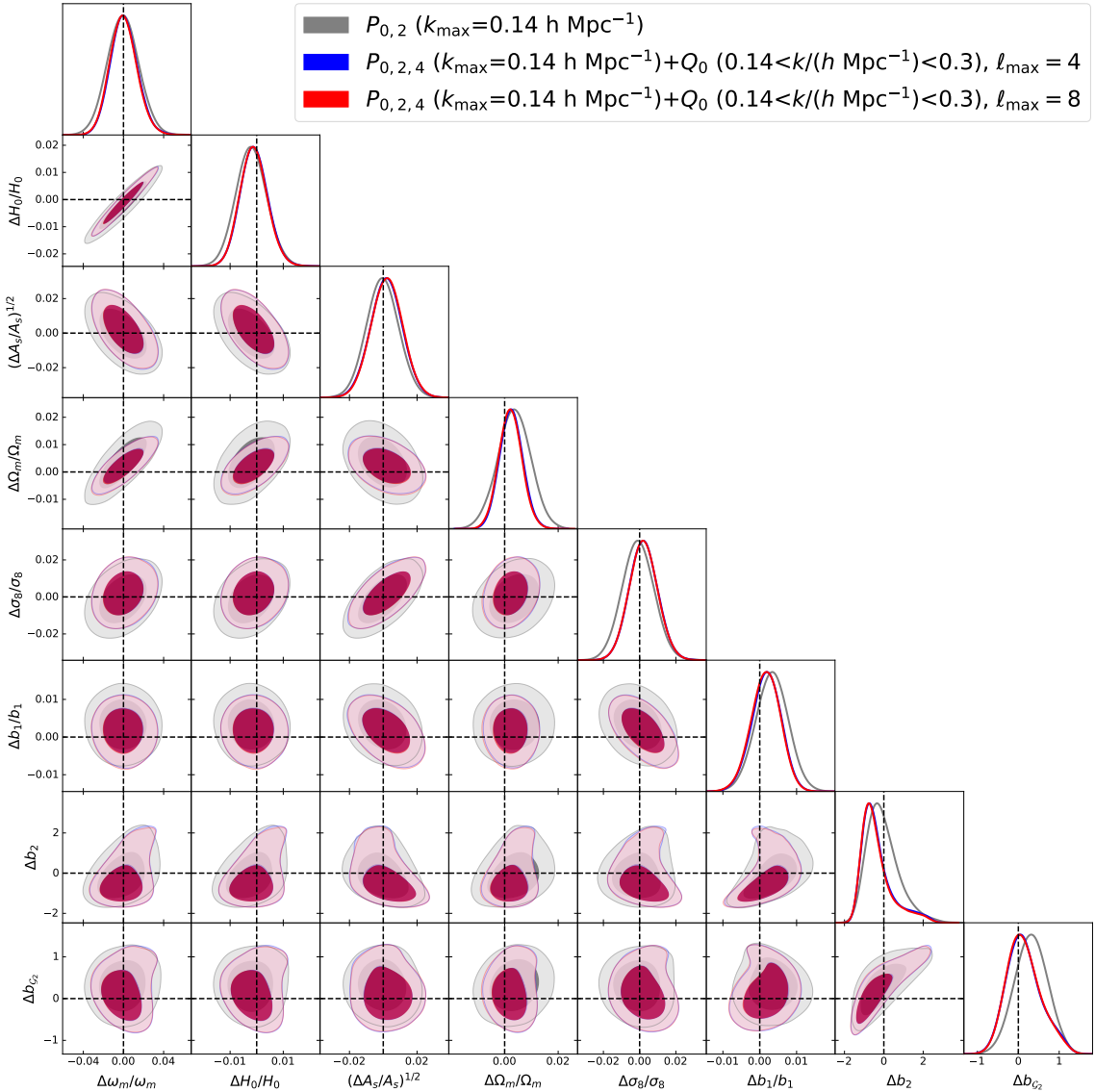
Figure 3. Posteriors from the PT challenge data for the analysis with fixed Ω_b/Ω_m and n_s.

4.2 Cosmological constraints with the ω_b prior

The information gain from Q_0 depends on the adopted priors and particular cosmological model. To illustrate this, we re-fitted the mock power spectra fixing ω_b instead of Ω_b/Ω_m, which was the choice adopted in our previous analysis. This simulates the addition of ω_b prior, which is readily available in e.g. Planck or BBN. We additionally allow n_s to vary freely. The corresponding results are presented in Fig. 4 and in Tab. 2. We find that the fit to Q_0 is unbiased all the way up to $k_{\max} = 0.4\ h\mathrm{Mpc}^{-1}$. We also see that in the case of a single prior on ω_b the addition of Q_0 improves the constraints on all the remaining cosmological parameters roughly by a factor of two.

Parameter	$P_{0,2}$ ($k_{\max} = 0.14\ h\mathrm{Mpc}^{-1}$)	$P_\ell + Q_0$, $\ell_{\max} = 4$	$P_\ell + Q_0$, $\ell_{\max} = 8$
$\Delta H_0/H_0$	-0.0020 ± 0.0059	-0.00096 ± 0.0052	-0.0011 ± 0.0052
$\Delta A^{1/2}/A^{1/2}$	-0.0004 ± 0.0096	0.0019 ± 0.0093	0.0021 ± 0.0093
$\Delta\omega_m/\omega_m$	0.000 ± 0.016	$0.001^{+0.013}_{-0.014}$	$0.000^{+0.012}_{-0.014}$
$\Delta b_1/b_1$	0.0033 ± 0.0044	$0.0018^{+0.0041}_{-0.0037}$	0.0016 ± 0.0040
Δb_2	$-0.04^{+0.55}_{-0.96}$	$-0.33^{+0.31}_{-0.93}$	$-0.36^{+0.32}_{-0.90}$
$\Delta b_{\mathcal{G}_2}$	0.31 ± 0.41	$0.14^{+0.34}_{-0.50}$	$0.14^{+0.34}_{-0.49}$
$\Delta\Omega_m/\Omega_m$	0.0035 ± 0.0062	0.0025 ± 0.0043	0.0022 ± 0.0044
$\Delta\sigma_8/\sigma_8$	-0.0008 ± 0.0088	0.0021 ± 0.0079	0.0021 ± 0.0079

Table 1. Constraint on key cosmological and nuisance parameters from the PT challenge mock power spectra, obtained with fixed Ω_b/Ω_m and n_s as in Ref. [11]. P_ℓ denotes the datavector $\{P_0, P_2, P_4\}$ with $k_{\max} = 0.14\ h\mathrm{Mpc}^{-1}$. The second and third columns show results of the addition of Q_0 in the range $0.14 \leq k/(h\mathrm{Mpc}^{-1}) < 0.3$. In the third column we add mean priors on the multipole moments with $\ell = 6, 8$ to the theory model. Parameters in the upper group part of the table were varied directly, while the lower group are the derived parameters.

It is useful to compare our results with the case of the true real space galaxy power spectrum, using the same k ranges. To that end, we replace Q_0 with the actual real-space power spectrum P_{gg} extracted from the same PT Challenge simulations, and refit the data. The diagonal elements of the Gaussian covariance for P_{gg} are roughly 4 times smaller than similar elements of Q_0 for the same volume and shot noise. As a result of this small covariance, the one-loop perturbation theory fit to P_{gg} becomes biased beyond $k_{\max} = 0.2\ h\mathrm{Mpc}^{-1}$, which we adopt as a baseline data cut in this case. The resulted parameter limits are very similar to those obtained from our baseline Q_0 analysis at $k_{\max} = 0.4\ h\mathrm{Mpc}^{-1}$. This matches the expectation that the two statistics should be equivalent at the level of total information for appropriate data cuts.

5 Applications to realistic surveys

So far we have studied Q_0 in application to the PT Challenge mocks whose total volume is $566\ h^{-3}\mathrm{Gpc}^3$ at the effective redshift $z = 0.61$. Current and future surveys will have somewhat smaller volumes, therefore it is useful to test to what extent the real space power spectrum can improve cosmological parameter measurements from realistic surveys. We address this question in this section and analyze the spectroscopic data from BOSS and DESI-like mock catalogs.

Parameter	$P_{0,2}$, ($k_{\max} = 0.14$)	$P_\ell + Q_0$ ($k_{\max} = 0.4$)	$P_\ell + P_{\mathrm{gg}}$ ($k_{\max} = 0.2$)
$\Delta H_0/H_0$	-0.0036 ± 0.0032	-0.0004 ± 0.0019	-0.0029 ± 0.0022
$\Delta A^{1/2}/A^{1/2}$	0.016 ± 0.023	-0.005 ± 0.013	$0.014^{+0.011}_{-0.012}$
$\Delta\omega_{cdm}/\omega_{cdm}$	-0.015 ± 0.020	0.008 ± 0.013	-0.0121 ± 0.0096
$\Delta n_s/n_s$	0.016 ± 0.022	-0.008 ± 0.011	0.014 ± 0.010
$\Delta b_1/b_1$	0.013 ± 0.014	-0.0024 ± 0.0066	0.0119 ± 0.0082
Δb_2	$0.25^{+0.70}_{-1.1}$	$-0.40^{+0.42}_{-0.66}$	$0.29^{+0.56}_{-1.0}$
$\Delta b_{\mathcal{G}_2}$	0.36 ± 0.40	$0.17^{+0.31}_{-0.39}$	$0.34^{+0.41}_{-0.37}$
$\Delta\Omega_m/\Omega_m$	-0.005 ± 0.013	0.0073 ± 0.0085	-0.0044 ± 0.0059
$\Delta\sigma_8/\sigma_8$	0.011 ± 0.018	-0.003 ± 0.010	$0.0110^{+0.0094}_{-0.011}$

Table 2. Constraints from the analysis of the PT challenge data with the ω_b prior. P_ℓ denotes the datavector $\{P_0, P_2, P_4\}$ with $k_{\max} = 0.14$ $h\mathrm{Mpc}^{-1}$. The second column shows results of the addition of Q_0 in the range $0.14 \leq k/(h\mathrm{Mpc}^{-1}) < 0.4$; while in the third column instead we add the actual real space power spectrum $P_{gg}(k)$ in the range $0.14 \leq k/(h\mathrm{Mpc}^{-1}) < 0.2$.

Parameter	P_ℓ	$P_\ell + Q_0$ ($\frac{k_{\max}}{h\mathrm{Mpc}^{-1}} = 0.3$)	$P_\ell + Q_0$ ($\frac{k_{\max}}{h\mathrm{Mpc}^{-1}} = 0.4$)
$H_0/(\mathrm{km/s/Mpc})$	$69.29^{+1.3}_{-1.6}$	$69.1^{+1.3}_{-1.4}$	$68.96^{+1.3}_{-1.4}$
$\ln(10^{10} A_s)$	$2.711^{+0.18}_{-0.2}$	$2.73^{+0.17}_{-0.2}$	$2.727^{+0.17}_{-0.2}$
ω_{cdm}	$0.1353^{+0.01}_{-0.014}$	$0.1327^{+0.0095}_{-0.013}$	$0.13^{+0.0091}_{-0.012}$
n_s	$0.9006^{+0.078}_{-0.081}$	$0.8922^{+0.068}_{-0.076}$	$0.9011^{+0.069}_{-0.074}$
Ω_m	$0.3383^{+0.018}_{-0.021}$	$0.3345^{+0.017}_{-0.02}$	$0.3298^{+0.016}_{-0.02}$
σ_8	$0.6644^{+0.039}_{-0.044}$	$0.6622^{+0.036}_{-0.044}$	$0.6568^{+0.036}_{-0.044}$

Table 3. Cosmological parameter constraints from the BOSS data with the ω_b prior. P_ℓ denotes the $\ell = 0, 2, 4$ moments in the range $0.01 \leq k/(h\mathrm{Mpc}^{-1}) < 0.2$, Q_0 is the real space power spectrum within $0.2 \leq k/(h\mathrm{Mpc}^{-1}) < 0.3$ (third column) or $0.2 \leq k/(h\mathrm{Mpc}^{-1}) < 0.4$ (fourth column).

5.1 BOSS survey

We apply now our method to the redshift space galaxy power spectrum measurement of the BOSS survey [9]. Using the `nbodykit` code [34], we measure the galaxy power spectrum multipoles of the BOSS data from four independent data chunks: low-z ($z = 0.38$) north galactic cap (NGC), high-z ($z = 0.61$) NGC, low-z south galactic cap (SGC), high-z SGC [3, 9]. For each chunk we construct the likelihood as follows. We use the full P_0, P_2, P_4 moments up to $k_{\max} = 0.2$ $h\mathrm{Mpc}^{-1}$ and Q_0, estimated with $\ell_{\max} = 4$, in the ranges 0.2 $h\mathrm{Mpc}^{-1} \leq k < 0.3$ $h\mathrm{Mpc}^{-1}$ and 0.2 $h\mathrm{Mpc}^{-1} \leq k < 0.4$ $h\mathrm{Mpc}^{-1}$. We do not include additional BAO data, as in Refs. [6, 47, 48],
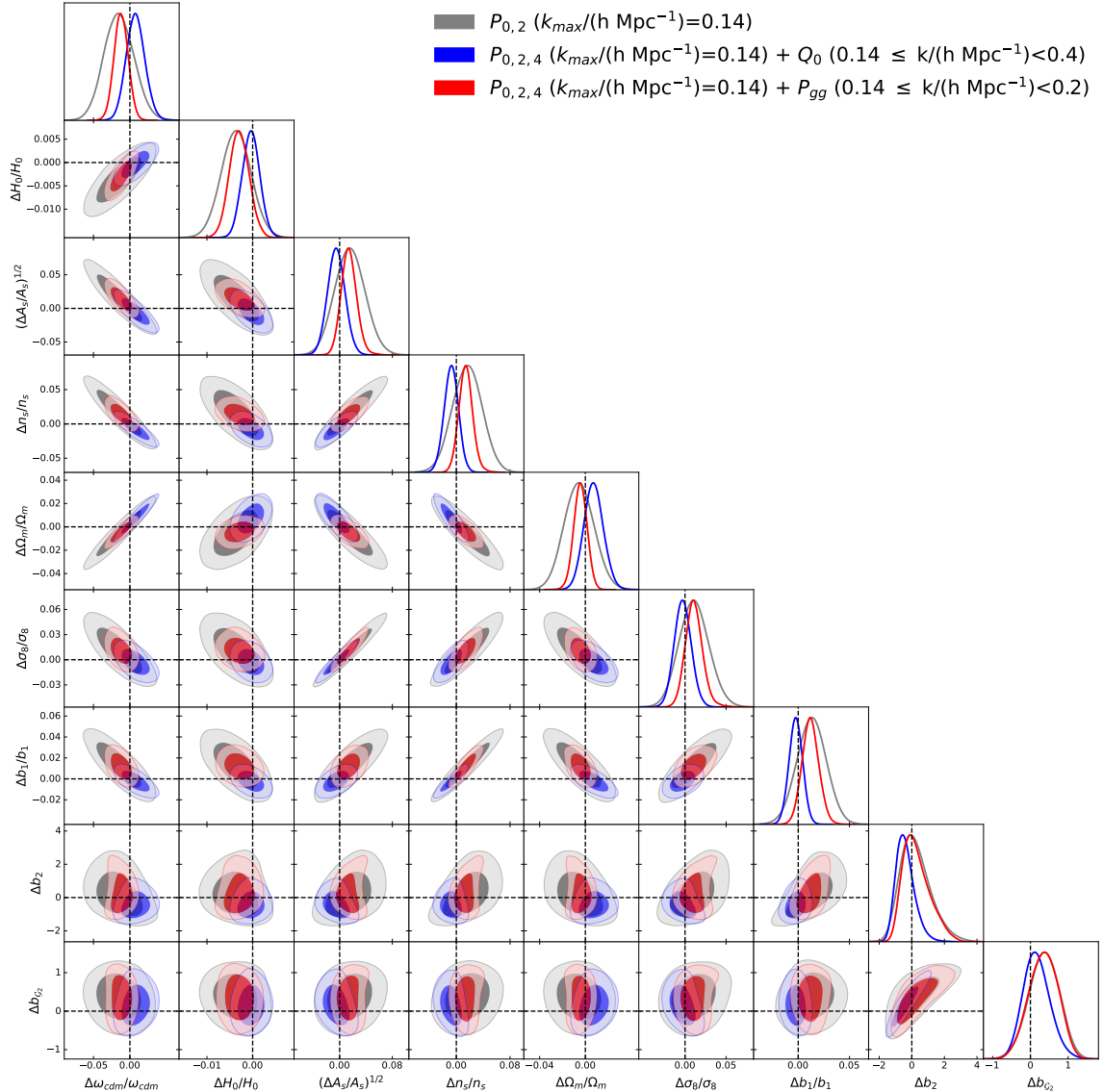
Figure 4. Posteriors from the analysis of the PT challenge mock galaxy power spectrum with a prior on ω_b.

because we want to clearly assess the improvement from Q_0 w.r.t. the usual multipoles analysis.

We fit parameters of the $\nu\Lambda$CDM model assuming three degenerate massive neutrinos with the total mass varied in the range $[0, 1]$ eV, and the BBN prior on the baryon density $\omega_b = 0.02258 \pm 0.0038$. We use the same priors on nuisance parameters as Ref. [47]. The covariance matrix for the full datavector is calculated using the empirical estimator based on 2048 Patchy mocks [49]. Our results for the joint fit of all four data chunks are displayed in Fig. 5 and in Table 3,[2] where we

---

[2]Only the parameters that are well constrained by the data, i.e. not dominated by priors, are
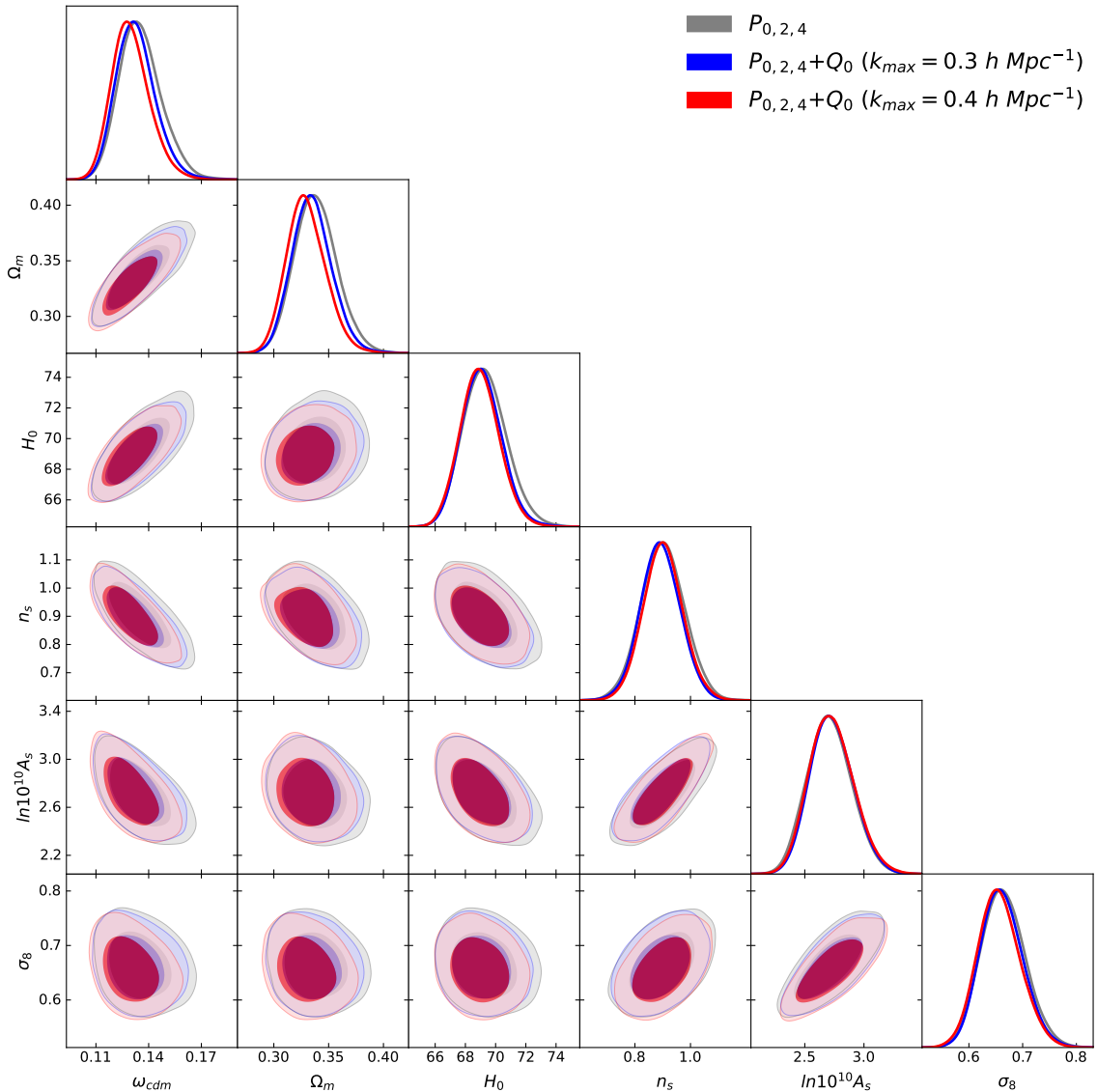
Figure 5. Posteriors from the cosmological analysis of the BOSS galaxy power spectrum measurements combined with the BBN prior on ω_b.

show results from the usual redshift-space multipoles alone and with Q_0, taken at $k_{\max} = 0.3\ h\mathrm{Mpc}^{-1}$ and $0.4\ h\mathrm{Mpc}^{-1}$.

In this case, the inclusion of Q_0 leads to somewhat marginal improvements of $\sim 10\%$, which are barely visible in the triangle plot. This is a result of a relatively large shot noise level of the BOSS galaxy sample, $\bar{n} \simeq (3-5) \cdot 10^3\ h^3\mathrm{Mpc}^{-3}$. In order to illustrate this, we may analyze mocks with lower shot noise, as appropriate for the upcoming DESI survey.

shown in this table.

5.2 DESI-like emission line galaxy mocks

In order to estimate the performance of our method for surveys such as Euclid and DESI, we apply it to the analysis of the mock emission line galaxy (ELG) catalogs from the extended Baryon Acoustic Oscillation Survey (eBOSS) survey [50]. An important aspect of these mocks is that they simulate the clustering of the ELGs, which exhibit a weaker fingers of God signature [48]. This factor suggests that the improvement from Q_0 may be somewhat less sizable than the improvement that we expect from the LRG samples.

Parameter	$P_{0,2}$	$P_\ell + Q_0, (k_{\max} = 0.3)$	$P_\ell + Q_0, (k_{\max} = 0.4)$
H_0	$71.86^{+0.53}_{-0.53}$	$71.03^{+0.51}_{-0.53}$	$71.1^{+0.52}_{-0.51}$
$\ln(10^{10}A_s)$	$3.005^{+0.076}_{-0.08}$	$3.106^{+0.07}_{-0.07}$	$3.113^{+0.069}_{-0.071}$
ω_{cdm}	$0.1215^{+0.0057}_{-0.0067}$	$0.1097^{+0.0043}_{-0.0051}$	$0.1093^{+0.0043}_{-0.0049}$
n_s	$0.9878^{+0.042}_{-0.039}$	$1.031^{+0.035}_{-0.035}$	$1.032^{+0.032}_{-0.032}$
b_1	$1.376^{+0.042}_{-0.041}$	$1.325^{+0.029}_{-0.031}$	$1.321^{+0.029}_{-0.031}$
Ω_m	$0.2789^{+0.0095}_{-0.011}$	$0.2622^{+0.0073}_{-0.0082}$	$0.2608^{+0.0071}_{-0.008}$
σ_8	$0.8308^{+0.021}_{-0.025}$	$0.8299^{+0.018}_{-0.02}$	$0.831^{+0.018}_{-0.02}$

Table 4. Constraints from the analysis of the Outer Rim mock data with the ω_b prior. We show only the parameters that are well constrained by the data. For P_ℓ the data cut is $k_{\max} = 0.2\,h\mathrm{Mpc}^{-1}$ in all analyses. For Q_0 we use the ranges $0.2\,h\mathrm{Mpc}^{-1} \le k < 0.3\,h\mathrm{Mpc}^{-1}$ (middle column) and $0.2\,h\mathrm{Mpc}^{-1} \le k < 0.4\,h\mathrm{Mpc}^{-1}$ (right column).

These eBOSS ELG mocks are based on the Outer Rim dark matter simulation [51], which were populated with ELG mock galaxies according to the eBOSS ELG clustering measurements [52]. We use the HOD-3 mock catalogs at $z = 0.865$. We measure the mock redshift space multipoles and analyze them as in Ref. [48]. The mocks have the following fiducial ΛCDM cosmology:

$$h = 0.71\,, \quad \omega_{cdm} = 0.1109\,, \quad \omega_b = 0.02258\,,$$
$$n_s = 0.963\,, \quad \sigma_8 = 0.8\,, \quad M_{\mathrm{tot}} = 0\ \mathrm{eV}\,. \tag{5.1}$$

We compare three different analyses: fits to $\ell = 0, 2$ moments at $k_{\max} = 0.2\,h\mathrm{Mpc}^{-1}$, fits to $\ell = 0, 2, 4$ moments at $k_{\max} = 0.2\,h\mathrm{Mpc}^{-1}$ and Q_0 for $0.2\,h\mathrm{Mpc}^{-1} \le k < 0.3\,h\mathrm{Mpc}^{-1}$, and fits to $\ell = 0, 2, 4$ moments at $k_{\max} = 0.2\,h\mathrm{Mpc}^{-1}$ and Q_0 for $0.2\,h\mathrm{Mpc}^{-1} \le k < 0.4\,h\mathrm{Mpc}^{-1}$. We compute the covariance in the Gaussian approximation using the true shot noise value $\bar{n} \simeq 5 \cdot 10^2\,h^3\mathrm{Mpc}^{-3}$ and the total volume of $V = 27\,h^{-3}\mathrm{Gpc}^3$, similar to the DESI ELG volume [53]. We use the same priors on nuisance parameters as in Ref. [48], but vary the spectral index n_s in the fit in addition to h, Ω_m and A_s. The physical baryon density ω_b is fixed to the fiducial value of the simulation.
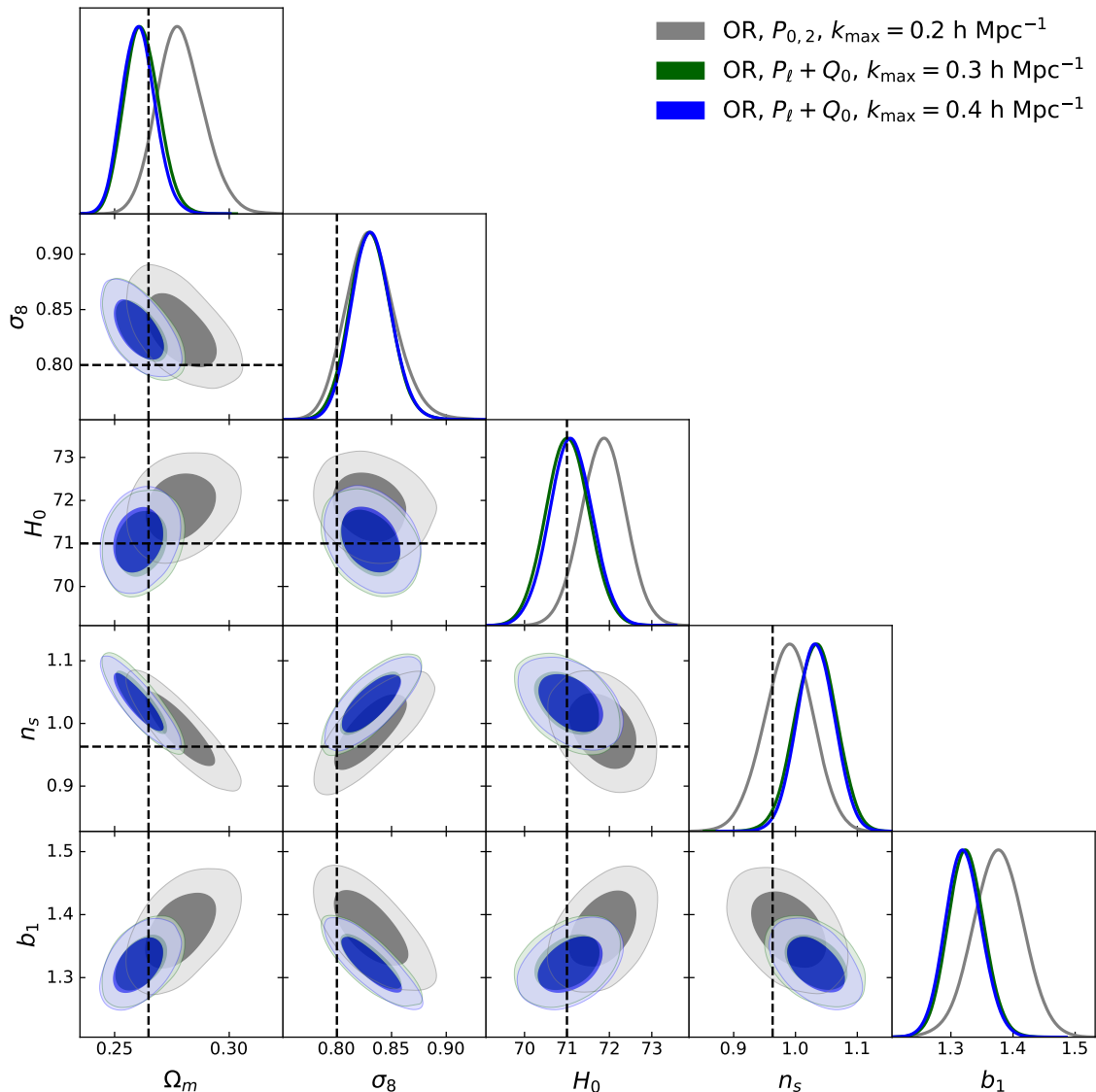
Figure 6. Posteriors from the cosmological analysis of the Outer Rim emission line galaxy mock power spectrum measurements.

Our results are show in Fig. 6 and in Table 4. The first important observation is that the recovery of Ω_m is somewhat biased in the $P_{0,2}$ analysis. This effect has been investigated in Ref. [48], suggesting that bias is likely a statistical fluctuation in a particular realization of the Outer Rim mocks. The second relevant observation is that this bias is largely removed after the inclusion of Q_0. This is accompanied with a $\sim 30\%$ shrinkage of the 1d marginalized contours for Ω_m and n_s. Note however that the bias in the full $\Omega_m - n_s$ plane is still present, giving hints of residual systematics in the simulation. The third important observation is that posteriors do not significantly shrink when the data cut for Q_0 is increased from 0.3 $h\mathrm{Mpc}^{-1}$ to 0.4 $h\mathrm{Mpc}^{-1}$. This implies that cosmological information in the real space power spectrum is limited

even for low shot noise samples.

All in all, we see that the improvement from Q_0 in the case of DESI-like mocks with high number density is quite significant. Therefore, the Q_0 statistic can be an important statistic for future surveys.

6   Discussion and Conclusions

In this paper we have proposed a new statistic, dubbed Q_0, which acts as a proxy for the real space power spectrum, and can be used to mitigate the impact of fingers of God. This can be easily constructed from the conventional redshift space power spectrum Legendre multipoles. We have shown how to perform such a reconstruction for an arbitrary survey and systematically include the information from higher-order Legendre multipoles if they carry non-negligible signal. Using our approach, Q_0 and its covariance matrix can be trivially computed from theory or mock catalogs, and included in the analysis at negligible extra cost. We have shown that the addition of Q_0 leads to notable improvements on cosmological constraints from mock catalogs, the amplitude of which varies within $(10-100)\%$ depending on survey characteristics, the choice of parameters, and priors in a particular analysis.

It is useful to compare Q_0 to the two-dimensional redshift space power spectrum $P(k, \mu)$. In terms of the signal-to-noise ratio, at $k_{\max} = 0.3 \ h\mathrm{Mpc}^{-1}$, the transverse moment Q_0 contains the same signal as $P(k, \mu)$ in the range $|\mu| \in [0, 0.3]$. Thus, we expect information gains from Q_0 to be roughly equivalent the corresponding μ-wedge. Given that the remaining μ-modes are quite sensitive to fingers-of-God, we expect that the $|\mu|$-range $[0.3, 1]$ contains very little, if any, viable cosmological information.

Crucially, Q_0 is more economic than $P(k, \mu)$, as it captures all relevant cosmological information in a relatively condensed datavector. This allows us to reduce the dimensionality of the total datavector compared to the $P(k, \mu)$ case; an effort which is of use if one wishes to avoid sampling noise biases if the covariance matrix is estimated from mock catalogs [54]. Alternative ways of avoiding this issue include analytic covariance matrix calculation [41, 55] or subspace-projection techniques [56].

The information gain from the addition of Q_0 for future surveys depends on several factors. First and foremost, it is dependent on the strength of FoG. The effect is large for the BOSS-like luminous red galaxies [3, 9] and the bright galaxy sample to be observed by DESI [53], though less so for emission line galaxies. Hence, we expect Q_0 to be particularly useful for the former galaxy selections.

The second factor determining the usefulness of Q_0 is the particular theoretical model chosen to fit the data, and adopted priors. We have found that within $\nu\Lambda\mathrm{CDM}$ the improvement from Q_0 increases when less restrictive priors are used and more free parameters are kept in the fit. Therefore, we expect even more information gain for models beyond $\Lambda\mathrm{CDM}$, e.g. for the early dark energy scenario (see e.g. [57] and

references therein), models with neutrino masses and additional relativistic degrees of freedom [4], axion dark matter cosmologies [58], or dynamical dark energy models [47, 59].

Our work can be extended in several ways. First, the transverse modes measured in a realistic survey can be contaminated by systematics [34, 48] so it is important to study to what extend this systematics can be mitigated in a realistic survey. Second, it would be interesting to see how much Q_0 can improve the constraints in combination with other techniques, such as the bispectrum and the BAO post-reconstruction information. This study can be performed for different tracers and within different cosmological models. Finally, it will interesting to work out an extension of our formalism to higher order statistics. We leave these research directions for future work.

Acknowledgments

A   General relation between moments and multipoles

The general relationship between power spectrum multipoles P_{2n} and moments Q_{2m} can be derived as follows. The power spectrum $P(k, \mu)$ can be represented by an expansion in even Legendre polynomials $\mathcal{L}_{2n}$ or in even powers of μ:

$$P(k, \mu) = \sum_{n=0}^{\infty} P_{2n}(k) \mathcal{L}_{2n}(\mu) \tag{A.1}$$

$$= \sum_{m=0}^{\infty} Q_{2m}(k) \mu^{2m} . \tag{A.2}$$

They are related by

$$P_{2n}(k) = \frac{4n+1}{2} \int_{-1}^{1} \mathrm{d}\mu \, P(k,\mu) \mathcal{L}_{2n}(\mu) \tag{A.3}$$

$$= \sum_{m=n}^{\infty} M_{nm} Q_{2m}(k), \tag{A.4}$$

where M is an upper triangular matrix given by

$$M_{nm} = \begin{cases} \frac{(4n+1)(2m)!}{2^{m-n}(m-n)!(2n+2m+1)!!}, & m \geq n, \\ 0, & \text{else} . \end{cases} \tag{A.5}$$

This follows by expressing powers of μ in terms of Legendre polynomials. If Eqs. (A.1) and (A.2) can be truncated at a finite $n_{\max} = m_{\max}$, then the equations relating moments and multipoles are a finite linear system of equations, and M is a $n_{\max} \times n_{\max}$ matrix. Under that assumption the moments in terms of multipoles are

$$\mathbf{Q}(k) = M^{-1}\mathbf{P}(k) \tag{A.6}$$

or explicitly

$$Q_{2m}(k) = \sum_{n=m}^{n_{\max}} (M^{-1})_{mn} P_{2n}(k) . \tag{A.7}$$

In particular, the μ^0 part of $P(k,\mu)$ is a sum over all nonzero multipoles,

$$Q_0(k) = \sum_{n=0}^{n_{\max}} (M^{-1})_{0n} P_{2n}(k) . \tag{A.8}$$

As discussed in the main text, care must be taken when the measured power spectrum multipoles are noisy.

References

[1] BOSS collaboration, F. Beutler et al., *The clustering of galaxies in the completed SDSS-III Baryon Oscillation Spectroscopic Survey: Anisotropic galaxy clustering in Fourier-space, Mon. Not. Roy. Astron. Soc.* **466** (2017) 2242 [1607.03150].

[2] A. Chudaykin and M. M. Ivanov, *Measuring neutrino masses with large-scale structure: Euclid forecast with controlled theoretical error, JCAP* **1911** (2019) 034 [1907.06666].

[3] M. M. Ivanov, M. Simonovic and M. Zaldarriaga, *Cosmological Parameters from the BOSS Galaxy Power Spectrum*, 1909.05277.

[4] M. M. Ivanov, M. Simonović and M. Zaldarriaga, *Cosmological Parameters and Neutrino Masses from the Final Planck and Full-Shape BOSS Data*, 1912.08208.

[5] T. Colas, G. D'amico, L. Senatore, P. Zhang and F. Beutler, *Efficient Cosmological Analysis of the SDSS/BOSS data from the Effective Field Theory of Large-Scale Structure*, *JCAP* **06** (2020) 001 [1909.07951].

[6] O. H. E. Philcox, M. M. Ivanov, M. Simonović and M. Zaldarriaga, *Combining Full-Shape and BAO Analyses of Galaxy Power Spectra: A 1.6% CMB-independent constraint on H0*, 2002.04035.

[7] O. H. Philcox, B. D. Sherwin, G. S. Farren and E. J. Baxter, *Determining the Hubble Constant without the Sound Horizon: Measurements from Galaxy Surveys*, 2008.08084.

[8] N. Sailer, E. Castorina, S. Ferraro and M. White, *Cosmology at high redshift – a probe of fundamental physics*, 2106.09713.

[9] BOSS collaboration, S. Alam et al., *The clustering of galaxies in the completed SDSS-III Baryon Oscillation Spectroscopic Survey: cosmological analysis of the DR12 galaxy sample*, *Mon. Not. Roy. Astron. Soc.* **470** (2017) 2617 [1607.03155].

[10] J. C. Jackson, *Fingers of God: A critique of Rees' theory of primoridal gravitational radiation*, *Mon. Not. Roy. Astron. Soc.* **156** (1972) 1P [0810.3908].

[11] T. Nishimichi, G. D'Amico, M. M. Ivanov, L. Senatore, M. Simonovic, M. Takada et al., *Blinded challenge for precision cosmology with large-scale structure: results from effective field theory for the redshift-space galaxy power spectrum*, 2003.08277.

[12] G. D'Amico, J. Gleyzes, N. Kokron, D. Markovic, L. Senatore, P. Zhang et al., *The Cosmological Analysis of the SDSS/BOSS data from the Effective Field Theory of Large-Scale Structure*, 1909.05271.

[13] M. Schmittfull, M. Simonović, V. Assassi and M. Zaldarriaga, *Modeling Biased Tracers at the Field Level*, *Phys. Rev. D* **100** (2019) 043514 [1811.10640].

[14] A. Chudaykin, M. M. Ivanov, O. H. E. Philcox and M. Simonović, *Nonlinear perturbation theory extension of the Boltzmann code CLASS*, *Phys. Rev. D* **102** (2020) 063533 [2004.10607].

[15] E. A. Kazin, A. G. Sanchez and M. R. Blanton, *Improving measurements of H(z) and Da(z) by analyzing clustering anisotropies*, *Mon. Not. Roy. Astron. Soc.* **419** (2012) 3223 [1105.2037].

[16] BOSS collaboration, J. N. Grieb et al., *The clustering of galaxies in the completed SDSS-III Baryon Oscillation Spectroscopic Survey: Cosmological implications of the Fourier space wedges of the final sample*, *Mon. Not. Roy. Astron. Soc.* **467** (2017) 2085 [1607.03143].

[17] M. Tegmark, A. J. S. Hamilton and Y.-Z. Xu, *The Power spectrum of galaxies in the 2dF 100k redshift survey*, *Mon. Not. Roy. Astron. Soc.* **335** (2002) 887 [astro-ph/0111575].

[18] SDSS collaboration, M. Tegmark et al., *The 3-D power spectrum of galaxies from the SDSS*, *Astrophys. J.* **606** (2004) 702 [astro-ph/0310725].

[19] B. A. Reid, D. N. Spergel and P. Bode, *Luminous Red Galaxy Halo Density Field Reconstruction and Application to Large Scale Structure Measurements*, *Astrophys. J.* **702** (2009) 249 [`0811.1025`].

[20] A. J. S. Hamilton and M. Tegmark, *The Real space power spectrum of the PSCz survey from 0.01 to 300 h Mpc**-1*, *Mon. Not. Roy. Astron. Soc.* **330** (2002) 506 [`astro-ph/0008392`].

[21] T. Baldauf, M. Mirbabayi, M. Simonović and M. Zaldarriaga, *LSS constraints with controlled theoretical uncertainties*, `1602.00674`.

[22] A. Chudaykin, M. M. Ivanov and M. Simonović, *Optimizing large-scale structure data analysis with the theoretical error likelihood*, *Phys. Rev. D* **103** (2021) 043525 [`2009.10724`].

[23] T. Brinckmann and J. Lesgourgues, *MontePython 3: boosted MCMC sampler and other features*, *Phys. Dark Univ.* **24** (2019) 100260 [`1804.07261`].

[24] B. Audren, J. Lesgourgues, K. Benabed and S. Prunet, *Conservative Constraints on Early Cosmology: an illustration of the Monte Python cosmological parameter inference code*, *JCAP* **1302** (2013) 001 [`1210.7183`].

[25] A. Lewis, *GetDist: a Python package for analysing Monte Carlo samples*, `1910.13970`.

[26] N. Kaiser, *Clustering in real space and in redshift space*, Mon. Not. Roy. Astron. Soc. **227** (1987) 1.

[27] L. Senatore and M. Zaldarriaga, *Redshift Space Distortions in the Effective Field Theory of Large Scale Structures*, `1409.1225`.

[28] M. Lewandowski, L. Senatore, F. Prada, C. Zhao and C.-H. Chuang, *EFT of large scale structures in redshift space*, *Phys. Rev. D* **97** (2018) 063526 [`1512.06831`].

[29] A. Perko, L. Senatore, E. Jennings and R. H. Wechsler, *Biased Tracers in Redshift Space in the EFT of Large-Scale Structure*, `1610.09321`.

[30] D. Baumann, A. Nicolis, L. Senatore and M. Zaldarriaga, *Cosmological Non-Linearities as an Effective Fluid*, *JCAP* **1207** (2012) 051 [`1004.2488`].

[31] J. J. M. Carrasco, M. P. Hertzberg and L. Senatore, *The Effective Field Theory of Cosmological Large Scale Structures*, *JHEP* **09** (2012) 082 [`1206.2926`].

[32] K. Yamamoto, M. Nakamichi, A. Kamino, B. A. Bassett and H. Nishioka, *A Measurement of the quadrupole power spectrum in the clustering of the 2dF QSO Survey*, *Publ. Astron. Soc. Jap.* **58** (2006) 93 [`astro-ph/0505115`].

[33] R. Scoccimarro, *Fast Estimators for Redshift-Space Clustering*, *Phys. Rev. D* **92** (2015) 083532 [`1506.02729`].

[34] N. Hand, Y. Li, Z. Slepian and U. Seljak, *An optimal FFT-based anisotropic power spectrum estimator*, *JCAP* **07** (2017) 002 [`1704.02357`].

[35] C. Alcock and B. Paczynski, *An evolution free test for non-zero cosmological*

constant, *Nature* **281** (1979) 358.

[36] M. M. Ivanov and S. Sibiryakov, *Infrared Resummation for Biased Tracers in Redshift Space*, *JCAP* **1807** (2018) 053 [1804.05080].

[37] T. Baldauf, M. Mirbabayi, M. Simonović and M. Zaldarriaga, *Equivalence Principle and the Baryon Acoustic Peak*, *Phys. Rev.* **D92** (2015) 043514 [1504.04366].

[38] D. Blas, S. Floerchinger, M. Garny, N. Tetradis and U. A. Wiedemann, *Large scale structure from viscous dark matter*, *JCAP* **1511** (2015) 049 [1507.06665].

[39] D. Blas, M. Garny, M. M. Ivanov and S. Sibiryakov, *Time-Sliced Perturbation Theory II: Baryon Acoustic Oscillations and Infrared Resummation*, *JCAP* **1607** (2016) 028 [1605.02149].

[40] A. Vasudevan, M. M. Ivanov, S. Sibiryakov and J. Lesgourgues, *Time-sliced perturbation theory with primordial non-Gaussianity and effects of large bulk flows on inflationary oscillating features*, *JCAP* **09** (2019) 037 [1906.08697].

[41] D. Wadekar, M. M. Ivanov and R. Scoccimarro, *Cosmological constraints from BOSS with analytic covariance matrices*, *Phys. Rev. D* **102** (2020) 123521 [2009.00622].

[42] M. Schmittfull, M. Simonović, M. M. Ivanov, O. H. E. Philcox and M. Zaldarriaga, *Modeling Galaxies in Redshift Space at the Field Level*, *JCAP* **05** (2021) 059 [2012.03334].

[43] V. Desjacques, D. Jeong and F. Schmidt, *Large-Scale Galaxy Bias*, *Phys. Rept.* **733** (2018) 1 [1611.09787].

[44] M. M. Abidi and T. Baldauf, *Cubic Halo Bias in Eulerian and Lagrangian Space*, *JCAP* **1807** (2018) 029 [1802.07622].

[45] T. Baldauf, U. s. Seljak, R. E. Smith, N. Hamaus and V. Desjacques, *Halo stochasticity from exclusion and nonlinear clustering*, *Phys. Rev. D* **88** (2013) 083507 [1305.2917].

[46] M. M. Ivanov, *to appear*, 2109.xxxxx.

[47] A. Chudaykin, K. Dolgikh and M. M. Ivanov, *Constraints on the curvature of the Universe and dynamical dark energy from the Full-shape and BAO data*, *Phys. Rev. D* **103** (2021) 023507 [2009.10106].

[48] M. M. Ivanov, *Cosmological constraints from the power spectrum of eBOSS emission line galaxies*, 2106.12580.

[49] F.-S. Kitaura et al., *The clustering of galaxies in the SDSS-III Baryon Oscillation Spectroscopic Survey: mock galaxy catalogues for the BOSS Final Data Release*, *Mon. Not. Roy. Astron. Soc.* **456** (2016) 4156 [1509.06400].

[50] S. Alam et al., *The Completed SDSS-IV extended Baryon Oscillation Spectroscopic Survey: N-body Mock Challenge for the eBOSS Emission Line Galaxy Sample*, 2007.09004.

[51] K. Heitmann et al., *The Outer Rim Simulation: A Path to Many-Core*

Supercomputers, Astrophys. J. Suppl. **245** (2019) 16 [1904.11970].

[52] S. Avila et al., *The Completed SDSS-IV extended Baryon Oscillation Spectroscopic Survey: exploring the Halo Occupation Distribution model for Emission Line Galaxies, Mon. Not. Roy. Astron. Soc.* **499** (2020) 5486 [2007.09012].

[53] DESI collaboration, A. Aghamousa et al., *The DESI Experiment Part I: Science,Targeting, and Survey Design*, 1611.00036.

[54] W. J. Percival et al., *The Clustering of Galaxies in the SDSS-III Baryon Oscillation Spectroscopic Survey: Including covariance matrix errors, Mon. Not. Roy. Astron. Soc.* **439** (2014) 2531 [1312.4841].

[55] D. Wadekar and R. Scoccimarro, *The Galaxy Power Spectrum Multipoles Covariance in Perturbation Theory*, 1910.02914.

[56] O. H. E. Philcox, M. M. Ivanov, M. Zaldarriaga, M. Simonovic and M. Schmittfull, *Fewer Mocks and Less Noise: Reducing the Dimensionality of Cosmological Observables with Subspace Projections, Phys. Rev. D* **103** (2021) 043508 [2009.03311].

[57] M. M. Ivanov, E. McDonough, J. C. Hill, M. Simonović, M. W. Toomey, S. Alexander et al., *Constraining Early Dark Energy with Large-Scale Structure*, 2006.11235.

[58] A. Laguë, J. R. Bond, R. Hložek, K. K. Rogers, D. J. E. Marsh and D. Grin, *Constraining Ultralight Axions with Galaxy Surveys*, 2104.07802.

[59] G. D'Amico, L. Senatore and P. Zhang, *Limits on wCDM from the EFTofLSS with the PyBird code, JCAP* **01** (2021) 006 [2003.07956].